

Difference in the nonlinear optical response of epitaxial Si on Ge(100) grown from SiH₄ at 500 °C and from Si₃H₈ at 350 °C due to segregation of Ge

V. K. Valev,^{1(a)} F. E. Leys,² M. Caymax,² and T. Verbiest¹

¹Institute for Nanoscale Physics and Chemistry (INPAC), Molecular and Nanomaterials, Katholieke Universiteit Leuven, Celestijnenlaan 200 D, B-3001 Leuven, Belgium

²IMEC vzw, Kapeldreef 75, 3001 Leuven, Belgium

(Received 3 December 2008; accepted 18 January 2009; published online 13 February 2009)

The properties of epitaxial strained Si on Ge (001) grown from SiH₄ at 500 °C and from Si₃H₈ at 350 °C have been investigated as a function of film thickness using second harmonic generation (SHG). A clear difference in the corresponding signal amplitude, for both the interface and the “bulk” contributions, is observed. After analysis of the nonlinear susceptibility tensor components, this difference is attributed to the segregation of Ge to the SiO₂/Si interface. It is demonstrated that when employed in combination with more standard experimental techniques, SHG can be a valuable tool for probing and characterizing the SiO₂/Si/Ge interfaces. © 2009 American Institute of Physics. [DOI: 10.1063/1.3082092]

Germanium is currently investigated for the replacement of silicon, in order to overcome the technological and fundamental limits associated with improving the performance of integrated circuits in Si. The main advantages of Ge over Si are its higher charge carrier mobility and its smaller band gap, which allows lower supply voltages. These advantages make this material very attractive for the integration of Ge-based metal-oxide-semiconductor field effect transistors (MOSFETs) into advanced devices.

However, generally speaking, GeO₂ displays a poorer quality compared to SiO₂, requiring a proper passivation of the Ge surface, before the deposition of the gate dielectric. A promising route for the passivation of Ge is the deposition of an ultrathin epitaxial Si layer on the surface, which is partly oxidized at low temperature prior to the deposition of the dielectric.¹

The implementation and optimization of this method requires the use of an experimental technique capable of observing and characterizing the properties of the buried thin film and its interfaces. The interface sensitive technique of the second harmonic generation (SHG) has been widely used in the past to characterize semiconductor materials especially Si.² Furthermore, while investigating the Pockels effect, many SHG studies have been done on Si_mGe_n superlattices. Consequently, we have applied SHG to the study of Ge/Si/SiO₂ layered systems, where Si is an ultrathin epitaxial film grown on Ge from SiH₄ at 500 °C and from Si₃H₈ at 350 °C, and SiO₂ is the native oxide grown in air. In this letter, we report a very different SHG response from samples grown from SiH₄ at 500 °C and from Si₃H₈ at 350 °C. This result is discussed in terms of the different possible contributions to the SHG signal and it is attributed to different amounts of segregation of Ge in the Si for the two different types of samples. We demonstrate that, when used in combination with other more established experimental techniques, SHG can be a very useful tool for investigating the materials of future integrated circuits.

A schematic diagram of the sample structure and of the measurement configuration is shown in Fig. 1. The samples were either 4 in. *p*-type Ge(100) wafers from Umicore [for the growth rate experiments and the secondary ion mass spectroscopy (SIMS) analysis] or 8 in. Ge on Si wafers provided by ASM (devices). Prior to deposition all wafers received a 2% HF-dip, followed by a de-ionized water rinse, and a dry under N₂ atmosphere. After loading at T ≤ 250 °C, a 10 minutes *in situ* bake in H₂ ambient at 650 °C was given to remove any remaining oxide. Growth from SiH₄ at 500 °C was done at a total pressure of 5.3 × 10³ Pa (40 torr), whereas growth from Si₃H₈ at 350 °C was done at atmospheric pressure to maximize the growth rate at this low temperature. In both cases, N₂ was used as a carrier gas. All depositions were done in an ASM Epsilon@2000 reactor. The Si thickness of these very thin layers was calculated from the Si dose as obtained from direct total reflection x-ray fluorescence.

The SHG measurements were performed using a QuantaRay laser at 1064 nm with a pulse width of a few nanoseconds and a repetition rate of 10 Hz. The incident beam went through a polarizer and then through a half wave plate, before reaching the sample. Furthermore, a 700 nm high pass filter ensured that any SHG generated in the optical elements preceding the sample was prevented from propagating toward the detector. The incidence angle θ was 45°. The SH signal generated from the sample at 532 nm was filtered by a 5 mm thick 900 nm low pass filter and, after going through

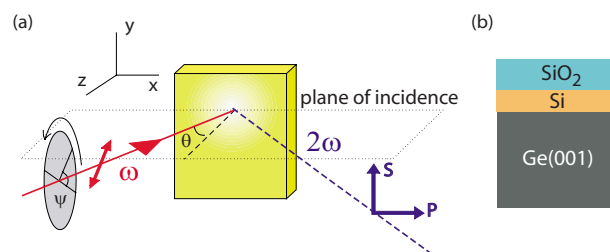


FIG. 1. (Color online) The schematic diagram of the experiment (a). The sample structure (b).

^aElectronic mail: v.k.valev@fys.kuleuven.be.

the analyzer, was detected by a photomultiplier tube on the entrance of which a 532 nm band pass filter with a width of 4 nm was placed.

In the following, the terms “*P*-polarized” and “*S*-polarized” light designate a linear polarization along the plane of optical incidence and perpendicular to it, respectively. By “polarization rotation angle” we indicate a direction of linear light polarization at a certain angle from the *P*-polarized or *S*-polarized light.

The nonlinear optical polarization $\mathbf{P}(2\omega)$ at the double frequency ω of incident light can be written in the following form:^{2,3}

$$\mathbf{P}(2\omega) = (\delta - \beta - 2\gamma)(\mathbf{E} \cdot \nabla)\mathbf{E} + \beta\mathbf{E}(\nabla \cdot \mathbf{E}) + \gamma\nabla(\mathbf{E} \cdot \mathbf{E}) + \zeta \sum_i \hat{e}_i \mathbf{E}_i \nabla_i \mathbf{E}_i, \quad (1)$$

where, for simplicity of the notation, we have omitted the frequency dependence on the electric fields $\mathbf{E}(\omega)$. In Eq. (1), the sum is over the crystallographic directions of the medium, \hat{e}_i are the corresponding unit vectors and, δ , β , γ , and ζ are phenomenological constants related to the symmetry of the sample. If we consider a single plane wave excitation, the first term is zero since we can write $(\mathbf{E} \cdot \nabla) \sim -i(\mathbf{E} \cdot \mathbf{k})$, which is zero for a transverse electromagnetic wave, with \mathbf{k} being the wave vector of the source polarization. The second term is canceled out due to Maxwell’s equations. The third term only gives rise to *P*-polarized SH light and it is isotropic.⁴ The last term contributes to both the isotropic and the anisotropic part of SH light, in all polarization combinations.

Furthermore, for Si (001), within the dipole approximation, one can define an effective polarization $\mathbf{P}^{\text{eff}}(2\omega)$, which describes the SHG response from surfaces and interfaces of centrosymmetric materials as

$$\begin{pmatrix} P_x^{\text{eff}} \\ P_y^{\text{eff}} \\ P_z^{\text{eff}} \end{pmatrix} = \begin{pmatrix} 0 & 0 & 0 & 0 & \chi_{xxz} & 0 \\ 0 & 0 & 0 & \chi_{yyz} & 0 & 0 \\ \chi_{zxx} & \chi_{zyy} & \chi_{zzz} & 0 & 0 & 0 \end{pmatrix} \begin{pmatrix} E_x^2 \\ E_y^2 \\ E_z^2 \\ 2E_y E_z \\ 2E_x E_z \\ 2E_x E_y \end{pmatrix}, \quad (2)$$

where $\chi_{i,j,k}$ represents the nonlinear susceptibility tensor components, with i , j , and k being the Cartesian indices within the reference frame of the sample.

Since some polarization combinations are forbidden in Eq. (2), which is the surface and interface specific, it follows that, with the help of Eq. (1), one can in principle separate the surface and the bulk contributions to the SHG signal, depending on the polarizer-analyzer combination. In this context, the term bulk refers to the material thickness in monolayers between the surface and the interfaces.

Figure 2 shows the SHG intensity along *S* [Figs. 2(a) and 2(b)] and *P* [Figs. 2(c) and 2(d)], versus the angle of rotation of the incoming polarization for samples grown at 500 °C [Figs. 2(a) and 2(c)] and at 350 °C [Figs. 2(b) and 2(c)]. Several curves corresponding to different thicknesses of the Si layer are plotted. It is clear that the signal from the samples grown at 350 °C is much stronger than that of the samples grown at 500 °C, especially above 9 ML.

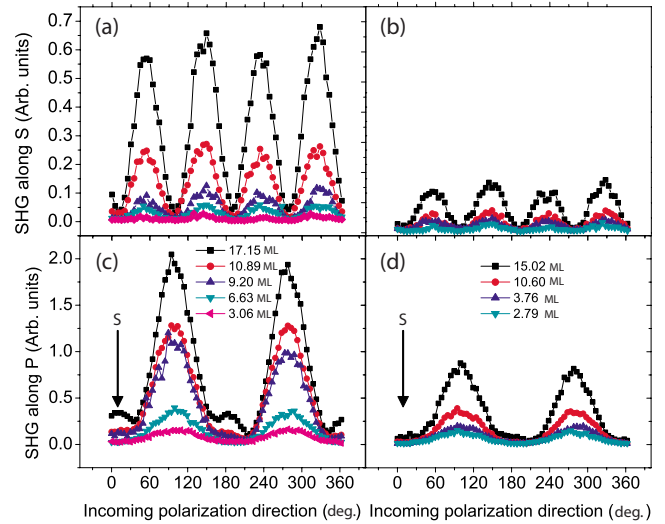


FIG. 2. (Color online) The SHG intensity as function of the angle of the incoming polarization, on one hand along *S* from samples grown at 350 °C (a) and at 500 °C (b) and on the other hand along *P* for samples grown at 350 °C (c) and at 500 °C (d).

From these graphs it is possible to extract the SHG response for all the relevant polarizer-analyzer combinations. In particular, we are interested in the *S*-*P* and the *S*-*S* data since, in the dipole approximation, the former addresses a single nonlinear susceptibility tensor component, which simplifies greatly the analysis, while the latter is forbidden. These results are shown in Figs. 3(a) and 3(b), respectively, where the lines are guides to the eye.

In both panels two different trends can be observed as function of thickness, below 7 ML the signals remain constant, while above there is an increase. This behavior is most likely attributable to the presence of native SiO_2 with a thickness of 4–7 ML. The subsequent increase can then be explained by the appearance of unoxidized Si layers. However, the increase in the SHG is sharper for the samples grown at 350 °C and it should be noted that the signal amplitude in the *S*-*P* configuration is much stronger than that of the *S*-*S* one. Since the latter is forbidden in the dipole approximation, it is the characteristic of a bulk response. More specifically, because this SH light is detected along *S*, the third term in Eq. (1) is canceled and the signal can be ascribed solely to $\zeta \sum_i \hat{e}_i \mathbf{E}_i \nabla_i \mathbf{E}_i$. In the *S*-*P* polarization combination, the SHG could be due to the χ_{zyy} nonlinear susceptibility tensor component in Eq. (2), as well as to the third and fourth terms in Eq. (1). In order to clarify this dependence, we analyzed the signal in the *P*-*S* configuration, which is also forbidden in

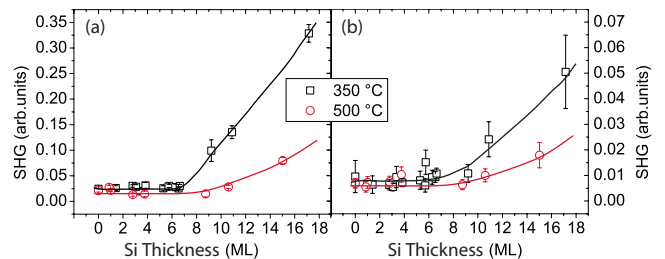


FIG. 3. (Color online) The SHG intensity as function of the thickness of deposited Si in monolayers, in the *S*-*P* polarizer-analyzer combination (a) and in the *S*-*S* polarizer-analyzer combination (b).

the dipole approximation but contains both last terms in Eq. (1). We found that the P - S curve is identical to the S - S one [see Fig. 3(b)], proving that the contribution of $\gamma \nabla(\mathbf{E} \cdot \mathbf{E})$ is negligible with respect to that of $\zeta \sum_i \hat{e}_i \mathbf{E}_i \nabla_i \mathbf{E}_i$. Therefore, we

can conclude that the signal in the S - P configuration is mainly due to χ_{zyy} , i.e., it originates from the SiO_2 surface and the Si interfaces of the sample. Consequently, it can be said that, above 7 ML, the increase in the SHG with respect to thickness is not only sharper for the samples grown at 350 °C but moreover it is much sharper for the interface specific contributions than for those of the bulk. This is an important point regarding the interface sensitivity of SHG in the case of Si/Ge studies.

Because of the particular thickness dependence of the SHG signal and the fact that the effect which we wish to understand is present at both the interfaces and in the bulk, several possible explanations can be ruled out, such as interface roughness,⁵ appearance of crystalline SiO_2 ,⁶ bonding across the interfaces,⁷ and processing step dependence (including H-termination, temperature annealing, and oxidation conditions). Charge transfer between the different film layers could in principle also contribute to the generated SH light⁸ however, since our signals are time-independent, we can eliminate this hypothesis. Under the influence of high power laser pulses, an electron-hole plasma can be created, disorder and melting can be induced, the temperature of the substrate can be risen, and a laser-induced annealing can be observed. All of these phenomena can lead to observable changes in the SHG intensity. In our case, varying the incident laser power did not affect any of the trends under discussion. Miscalculation at the crystal surface of materials has also been shown to affect the SHG response, yet the miscut angle in our samples is very small and no significant macroscopic net step structure can be present. Additionally, an azimuthal rotation of the sample revealed an isotropic SHG response and not the one-fold signature of steps. A 4% lattice mismatch between Ge and Si causes the appearance of strain in the monolayers of Si closest to Ge. The effects of strain on the SH signal have been studied many times⁹ and, furthermore, strain affects both the interfaces and the bulk. However, because the dislocation energy at the Ge surface is very low, after the seventh monolayer it is expected that the strain would relax through dislocations. Assuming that the initial 4–7 ML are oxidized, the strain is then expected to disappear after 11–14 MLs. However, in Fig. 3 it can be seen that there is no drastic change in the trends above 14 MLs. Finally, another possible explanation is the segregation of Ge in the Si layers, which has been shown by Leys *et al.*¹⁰ The authors demonstrated that Ge segregation occurs during the deposition of the Si film, which results in a clear peak in the SIMS data at the surface. This surface concentration is in agreement with the fact that we observe stronger signals from the interfaces than from the bulk in SHG. Furthermore, the concentration of Ge at the surface of Si was found by Leys *et al.*¹⁰ to be much smaller for the samples grown at 350 °C than from those grown at 500 °C. This variation in concentration can

indeed be responsible for the difference in the corresponding SHG intensities in Fig. 3. Finally, Leys *et al.*¹⁰ found a steeper indiffusion profile for the samples grown at 350 °C than for those at 500 °C. This means that the relative difference in Ge concentration between these samples increases with thickness, which is in agreement with the increasing difference with thickness, above 7 ML, between the SHG signals in both Figs. 3(a) and 3(b). Below 7 ML, only SiO_2 is present on top of the Ge and since this material is transparent at the wavelengths that we use, its contribution is difficult to observe alone. However, it can become apparent once it starts affecting the interference between the larger signals from the Si interfaces.

In conclusion, we have investigated the thickness dependence of epitaxial Si on Ge (100) grown from SiH_4 at 500 °C and from Si_3H_8 at 350 °C with SHG. A clear difference in the SHG response of the samples is observed. After separating the interface from the bulk signals, we established that the difference in SHG most likely originates from the segregation of different amounts of Ge in the Si layers. Furthermore we found a larger SHG response from the interface than from the bulk. On one hand, this is due to the interface specificity of the SHG technique and on the other it is related to previously observed concentration of segregated Ge at the Si surface. It should be noted that the difference in surface/interface specific SHG is much larger than that of the SIMS peaks reported in Ref. 10. This demonstrates that, in combination with other techniques, SHG can be a very useful tool for probing the buried interfaces in Si/Ge systems.

Parts of this work have been supported by the INPAC research institute, the K.U. Leuven, the Belgian government, and the Flemish government. We wish to thank Rik Strobbe and Frans Hennau for their technical support.

¹D. P. Brunco, B. De Jaeger, G. Eneman, J. Mitard, G. Hellings, A. Satta, V. Terzieva, L. Souriau, F. E. Leys, G. Pourtois, M. Houssa, G. Winderickx, E. Vrancken, S. Sioncke, K. Opsmer, G. Nicholas, M. Caymax, A. Stesmans, J. Van Steenberghe, P. W. Mertens, M. Meuris, and M. M. Heyns, *J. Electrochem. Soc.* **155**, H552 (2008).

²G. Lüpke, *Surf. Sci. Rep.* **35**, 75 (1999).

³J. F. McGilp, *Prog. Surf. Sci.* **49**, 1 (1995); D. L. Mills, *Nonlinear Optics Basic Concepts*, 2nd ed. (Springer, New York, 1998), p. 160.

⁴J. E. Sipe, V. Mizrahi, and G. I. Stegeman, *Phys. Rev. B* **35**, 9091 (1987).

⁵S. T. Cundiff, W. H. Knox, F. H. Baumann, K. W. Evans-Lutterodt, M.-T. Tang, M. L. Green, and H. M. van Driel, *Appl. Phys. Lett.* **70**, 1414 (1997).

⁶G. Lüpke, D. J. Bottomley, and H. M. van Driel, *Phys. Rev. B* **47**, 10389 (1993).

⁷G. Lüpke, C. Meyer, U. Emmerichs, F. Wolter, and H. Kurz, *Phys. Rev. B* **50**, 17292 (1994).

⁸J. Bloch, J. G. Mihaychuk, and H. M. van Driel, *Phys. Rev. Lett.* **77**, 920 (1996).

⁹J.-W. Jeong, S.-C. Shin, N. N. Dadoenkova, I. L. Lyubchanskii, V. K. Valev, and Th. Rasing, *Appl. Phys. Lett.* **90**, 044108 (2007).

¹⁰F. E. Leys, R. Bonzom, B. Kaczer, T. Janssens, W. Vandervorst, B. De Jaeger, J. Van Steenberghe, K. Martens, D. Hellin, J. Rip, G. Dillaway, A. Delabie, P. Zimmerman, M. Houssa, A. Theuwis, R. Loo, M. Meuris, M. Caymax, and M. M. Heyns, *Mater. Sci. Semicond. Process.* **9**, 679 (2006).